Cell

An ARGONAUTE4-Containing Nuclear Processing Center Colocalized with Cajal Bodies in *Arabidopsis thaliana*

Carey Fei Li,[1,2] Olga Pontes,[4] Mahmoud El-Shami,[5] Ian R. Henderson,[2] Yana V. Bernatavichute,[1,2] Simon W.-L. Chan,[2,6] Thierry Lagrange,[5] Craig S. Pikaard,[4] and Steven E. Jacobsen[1,2,3,*]
[1] Molecular Biology Institute
[2] Department of Molecular, Cell and Developmental Biology
[3] Howard Hughes Medical Institute
University of California, Los Angeles, Los Angeles, CA 90095, USA
[4] Biology Department, Washington University, 1 Brookings Drive, St. Louis, MO 63130, USA
[5] LGDP, UMR 5096, Université de Perpignan, 66860 Perpignan Cedex, France
[6] Present address: Section of Plant Biology, University of California, Davis, Davis, CA 95616, USA.
*Contact: jacobsen@ucla.edu
DOI 10.1016/j.cell.2006.05.032

SUMMARY

ARGONAUTE4 (AGO4) and RNA polymerase IV (Pol IV) are required for DNA methylation guided by 24 nucleotide small interfering RNAs (siRNAs) in *Arabidopsis thaliana*. Here we show that AGO4 localizes to nucleolus-associated bodies along with the Pol IV subunit NRPD1b; the small nuclear RNA (snRNA) binding protein SmD3; and two markers of Cajal bodies, trimethylguanosine-capped snRNAs and the U2 snRNA binding protein U2B″. AGO4 interacts with the C-terminal domain of NRPD1b, and AGO4 protein stability depends on upstream factors that synthesize siRNAs. AGO4 is also found, along with the DNA methyltransferase DRM2, throughout the nucleus at presumed DNA methylation target sites. Cajal bodies are conserved sites for the maturation of ribonucleoprotein complexes. Our results suggest a function for Cajal bodies as a center for the assembly of an AGO4/NRPD1b/siRNA complex, facilitating its function in RNA-directed gene silencing at target loci.

INTRODUCTION

Argonautes are PAZ- and PIWI-domain-containing proteins crucial to RNA interference (RNAi) pathways (Carmell et al., 2002). In RNAi, Argonaute proteins incorporate small interfering RNAs (siRNAs) made by Dicer enzymes and use the siRNAs as guides to target homologous sequences for gene silencing (Meister and Tuschl, 2004). RNAi-mediated gene silencing can occur posttranscriptionally through target RNA degradation or translation inhibition (Fagard et al., 2000; Hannon, 2002; Tijsterman et al., 2002) or at the transcription level by histone and/or DNA methylation (Chan et al., 2005; Verdel et al., 2004; Volpe et al., 2002; Wassenegger, 2005; Zilberman et al., 2003).

AGO4 from *Arabidopsis thaliana* was isolated as a suppressor of transcriptional gene silencing at the *SUPERMAN* (*SUP*) locus and was shown to be involved in a phenomenon termed RNA-directed DNA methylation (RdDM) (Chan et al., 2005; Wassenegger, 2005; Zilberman et al., 2003). The *ago4-1* mutant reduces DNA methylation at CNG and asymmetric sites (CHH, where H = A, T, or C) at loci such as *SUP*, *FWA*, *AtSN1*, 5S ribosomal genes (rDNA), and *MEA-ISR* and also decreases histone H3 lysine 9 methylation (Chan et al., 2004; Xie et al., 2004; Zilberman et al., 2003; Zilberman et al., 2004). The function of *AGO4* is locus specific since *ago4-1* showed no effect at the *CEN* and *Ta3* loci in pericentromeric heterochromatin (Zilberman et al., 2003). The *ago4-1* mutant also blocked de novo DNA methylation and silencing of an *FWA* transgene, demonstrating the role of AGO4 in the establishment of DNA methylation (Chan et al., 2004).

In addition to AGO4, several other factors are involved in RdDM, including the de novo DNA methyltransferase DOMAINS REARRANGED METHYLTRANSFERASE 2 (DRM2) and the RNA silencing components RNA-DEPENDENT RNA POLYMERASE 2 (RDR2) and DICER-LIKE 3 (DCL3) (Cao and Jacobsen, 2002; Chan et al., 2004; Xie et al., 2004). Recent evidence has also shown an important role for RNA polymerase IV (Pol IV) in transcriptional silencing (Chan et al., 2004; Herr et al., 2005; Kanno et al., 2005; Onodera et al., 2005; Pontier et al., 2005). Pol IV is a novel fourth class of DNA-dependent RNA polymerases in plants, with its largest subunit encoded by *NRPD1a* or *NRPD1b* and its second largest subunit encoded by *NRPD2a*. Since *nrpd1a* mutants eliminate siRNAs at many loci, while *nrpd1b* mutants do not, NRPD1a has been proposed to act upstream in the initial production of siRNAs, while

NRPD1b might act downstream in the targeting of DNA methylation (Kanno et al., 2005; Pontier et al., 2005).

Despite the important role that AGO4 plays in RdDM, little is known about its localization or interacting partners. Here we show that AGO4 localizes to a distinct nucleolus-associated body. We also found that NRPD1b localized with AGO4 and physically interacted with AGO4 through its large C-terminal domain. Mutations in the upstream RNAi components *DCL3*, *RDR2*, and *NRPD1a* eliminated AGO4 staining in the body, as well as reduced AGO4 protein levels overall, but mutations in factors that act downstream such as NRPD1b and DRM2 did not. This nuclear body does not colocalize with major target sites of AGO4 action or with the de novo DNA methyltransferase DRM2. Instead, the AGO4 nuclear body colocalizes with the snRNA binding protein SmD3 and two conserved markers of Cajal bodies, the trimethylguanosine cap of snRNAs and the U2 snRNA binding protein U2B″, strongly suggesting that the AGO4 bodies correspond to Cajal bodies. Cajal bodies serve as important centers for the maturation and processing of several ribonucleoparticles, which enter the Cajal body, are modified there, and then exit the Cajal body for utilization in processes elsewhere (Cioce and Lamond, 2005). The best studied example is snRNAs, which are posttranscriptionally modified and associate with specific proteins in Cajal bodies before their use in splicing elsewhere in the nucleus. We propose that the Cajal body plays an analogous function in the processing of transcripts during early steps of RNAi and the incorporation of the resulting siRNAs into an AGO4/NRPD1b/siRNA ribonucleoprotein complex that is utilized for RNA-directed DNA methylation at target loci.

RESULTS

AGO4 Localizes to a Distinct Nuclear Body

We constructed an N-terminally epitope-tagged *AGO4* transgene by engineering four copies of the Myc tag into a genomic complementing fragment of *AGO4* driven by its native promoter. The functionality of *myc-AGO4* was confirmed by its ability to restore silencing of the endogenous *SUP* locus in the *ago4-1 clk-st* mutant line (Cao and Jacobsen, 2002; Jacobsen and Meyerowitz, 1997; Zilberman et al., 2003). First-generation *myc-AGO4*-transformed *ago4-1 clk-st* plants displayed highly penetrant restoration of a silenced *SUP* floral phenotype of extra stamens and unfused carpels, indicating that the transgene is functional (Figure 1A). As a second verification of functionality, we showed that Myc-AGO4 restored RNA-directed asymmetric DNA methylation at *MEA-ISR* in the *ago4-1* mutant using a DNA methylation cutting assay (Zilberman et al., 2003) (Figure 1B). Western blot analysis of crude protein extract generated from a *myc-AGO4* plant showed a single band close to the predicted size of 110 kDa and no crossreactivity with other plant proteins (Figure 1C).

AGO4 was previously shown to be a nuclear-localized protein in transient expression assays in *Nicotiana benthamiana* leaves (Xie et al., 2004). We utilized c-Myc antibodies and fluorescence microscopy to examine AGO4 subnuclear localization when the protein was expressed from its native promoter. We identified two key localization patterns. First, AGO4 displayed a euchromatic localization throughout the nucleus that showed lower signal in DAPI staining chromocenters (Figure 1D). Chromocenters are highly condensed, heterochromatic DNA that contain centromeric and pericentromeric repeat sequences (Fransz et al., 2002). The exclusion of AGO4 from chromocenters is consistent with previous data demonstrating that *ago4-1* did not affect silencing at centromeric repeats or the pericentromeric *Ta3* locus (Zilberman et al., 2003). Instead, AGO4 is important for silencing at DNA methylated loci found in otherwise euchromatic regions such as *SUP* and *FWA*, both of which are localized away from chromocenters (Chan et al., 2004; Soppe et al., 2002; Tran et al., 2005; Zilberman et al., 2003).

Second, immunofluorescence analysis showed that AGO4 localized to a distinct body either adjacent to or within the nucleolus (Figure 1D; see also Table S1 in the Supplemental Data available with this article online). In a small fraction of nuclei, we observed a second or third AGO4 body, usually associated with additional nucleoli (8%, n = 168) (see examples in figures and Table S1). To test whether the AGO4 body might correspond to one of the chromocenters, we performed DNA fluorescence in situ hybridization (DNA-FISH) with a probe that recognizes the 180 base pair centromeric repeat sequences (*CEN*) and hybridizes to all of the chromocenters (Fransz et al., 2002). We found that the AGO4 nuclear bodies did not colocalize with centromeric repeats (Figure 1E), suggesting that they are not chromocenters.

The *ago4-1* mutant shows reduced histone H3 lysine 9 dimethylation (H3K9me2) at AGO4 target loci such as *SUP* and *AtSN1* (Zilberman et al., 2004). To test whether the AGO4 body might be a site of concentrated H3K9me2 targeting, we stained nuclei with an antibody specific for H3K9me2. The AGO4 body did not stain with H3K9me2 (Figure 2A). Furthermore, localization of Myc-AGO4 and H3K9me2 were anticorrelated, likely reflecting the fact that most H3K9me2 resides in chromocenters (Soppe et al., 2002) while a lower amount of H3K9me2 is found at scattered silent loci in euchromatin (Johnson et al., 2002; Zilberman et al., 2003). We also examined the colocalization of AGO4 with trimethylated lysine 27 of histone H3 (H3K27me3), a mark of genes silenced by Polycomb group proteins that reside outside of chromocenters (Chanvivattana et al., 2004; Lindroth et al., 2004; Mathieu et al., 2005) (Figure 2A). We found that the AGO4 body did not stain with H3K27me3 and that the AGO4 signal outside of the nuclear body was generally similar to that of H3K27me3, in that both were concentrated outside of DAPI staining chromocenters.

RNA Silencing Mutants Disrupt AGO4 Localization and Stability

To test whether the localization of AGO4 is dependent on upstream RNAi components, we crossed Myc-AGO4 into

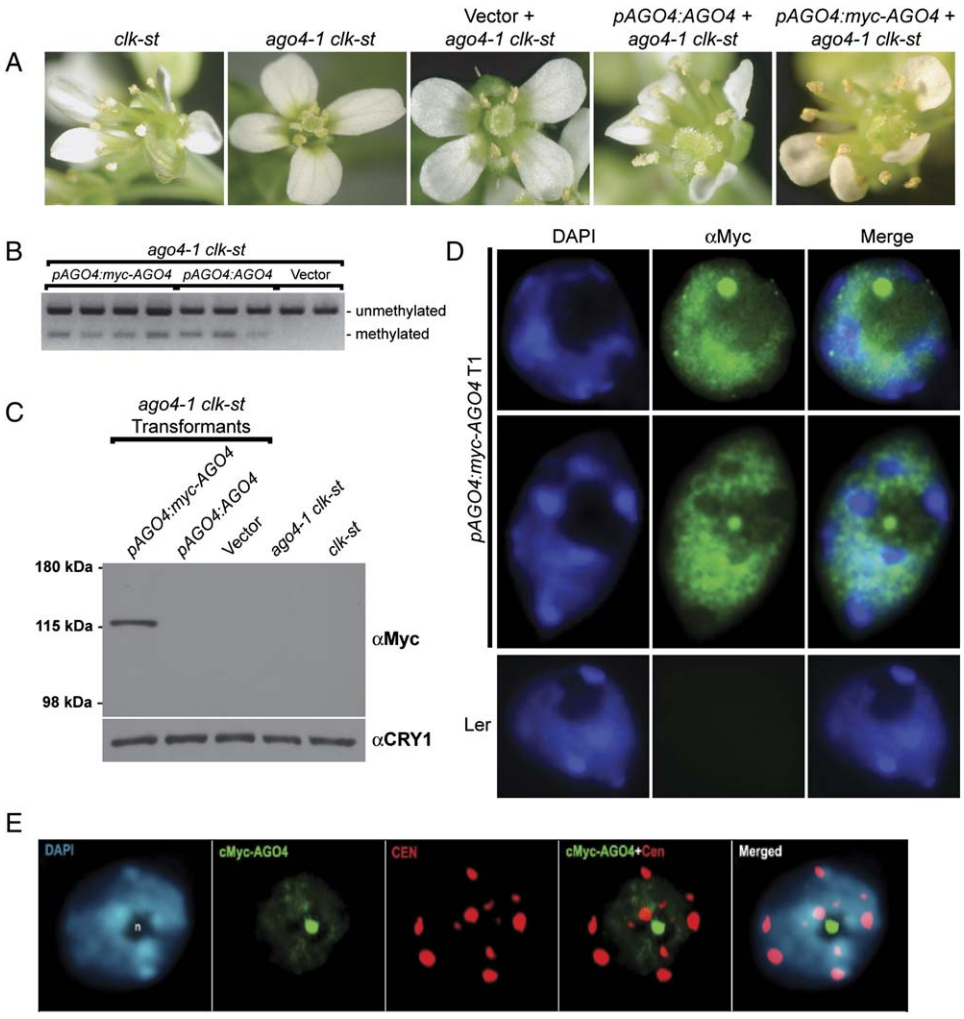

Figure 1. Myc-Tagged AGO4 Is Localized to a Nucleolar-Associated Body

(A) Complementation of the *ago4-1 clk-st* mutant by *myc-AGO4*. Flowers from first-generation transformants were scored for the reappearance of the *SUP* phenotype of extra stamens and unfused carpels.

(B) Complementation of *ago4-1* using a *MEA-ISR* bisulfite cutting assay. Sodium bisulfite modification of genomic DNA destroys a BamHI restriction site at *MEA-ISR* unless DNA methylation is present to prevent modification. Following PCR, the generation of a lower BamHI-digested band thus indicates the presence of DNA methylation at this asymmetric cytosine. An *ago4-1* mutant transformed with vector alone revealed no methylation, but *AGO4* transgenes complement and show reappearance of DNA methylation.

(C) Western blot analysis of Myc-AGO4 from crude protein preparations. The photoreceptor protein CRY1 was used as a loading control (Lin et al., 1996).

(D) Fluorescence microscopy analysis of Myc-AGO4 localization in *Arabidopsis* nuclei. Ler is the wild-type negative control containing no Myc-tagged AGO4.

(E) Localization of the Myc-AGO4 nucleolar body relative to the centromeric repeats (*CEN*) by DNA-FISH analysis.

homozygous *dcl3*, *rdr2*, or *dcl3 rdr2* double-mutant backgrounds. By fluorescence microscopy, both the nuclear body and euchromatic staining of AGO4 were dramatically reduced in *rdr2* and *dcl3 rdr2* double mutants (Figure 3A; Table S3). For *dcl3*, 61% of nuclei displayed a dramatic decrease in AGO4 levels, while the other 39% showed wild-type AGO4 levels (n = 70). It has been demonstrated previously that *dcl3* has weaker effects than *rdr2* on siRNA levels and DNA methylation (Chan et al., 2004; Xie et al., 2004). Thus, the difference between the two *dcl3* populations might be explained by either stochastic or cell-type-specific redundancy with other *DCL* genes (Schauer et al., 2002).

To determine whether the decrease of nuclear AGO4 was due to overall protein loss or a defect in AGO4 nuclear localization, a semiquantitative Western blot of crude protein extract from mutant plants was used to measure AGO4 levels (Figure 3B). Myc-AGO4 protein levels were decreased moderately in *dcl3* and severely in *rdr2* and *dcl3 rdr2* double mutants. These decreases were not due to transcriptional repression of the transgene since *myc-AGO4* transcripts were at similar levels in the various

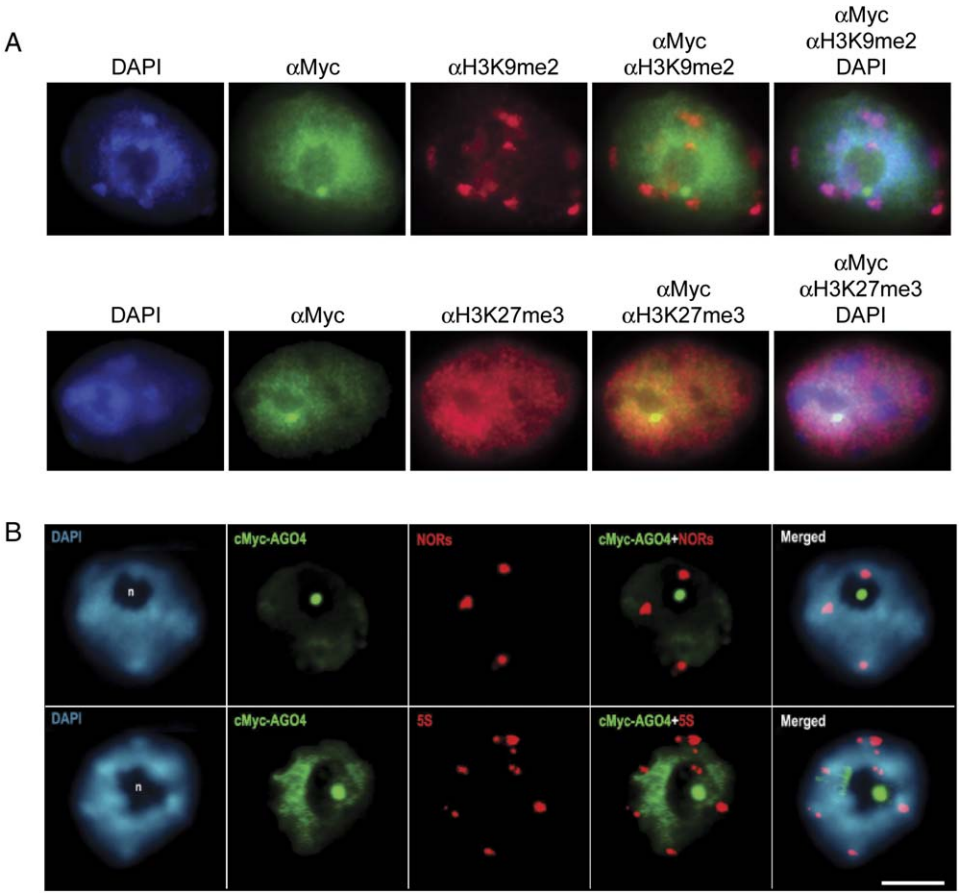

Figure 2. Localization of Myc-AGO4 Relative to Histone Modifications and rDNA Genes

(A) Fluorescence microscopy analysis showing Myc-AGO4 localization relative to H3K9me2 (top panel) or H3K27me3 (bottom panel).

(B) DNA-FISH analysis of the 45S rDNA (nucleolar organizer regions; NORs) or 5S rDNA genes relative to the Myc-AGO4 nuclear dot.

mutant and wild-type backgrounds (Figure 3C). In contrast to the RNA silencing mutants, a mutation in the DNA methyltransferase gene *DRM2*, which likely acts downstream of AGO4, had no effect on Myc-AGO4 localization or protein level (Figures 3D and 3B). These results suggest that the upstream components DCL3 and RDR2 are needed for stabilizing AGO4.

Since DRM2 is a downstream component in the AGO4-dependent RdDM pathway, it is possible that DRM2 might have the same localization pattern as AGO4. To investigate this, a 9× Myc-tagged genomic *DRM2* controlled by its native promoter was generated. We demonstrated functionality of the transgene by showing that it restored DNA methylation at *MEA-ISR* in a *drm2* mutant (Figure 3E). By fluorescence microscopy, DRM2 showed a euchromatic localization that was reduced in DAPI staining chromocenters in a manner analogous to AGO4. However, unlike Myc-AGO4, DRM2-myc was not found in a distinct body near the nucleolus. These results are consistent with the idea that DRM2 acts with AGO4 at RdDM target loci but not in the AGO4 body.

AGO4 Colocalizes with the RNA Polymerase IV Subunit NRPD1b

We previously showed that a mutation in *NRPD1a* (*sde4*) blocked de novo DNA methylation of a newly introduced *FWA* transgene, resulting in overexpression of the transgene and a late-flowering phenotype (Cao and Jacobsen, 2002; Chan et al., 2004). This same defect in establishment of DNA methylation was seen in *ago4-1*, *dcl3*, and *rdr2* mutants. We asked whether NRPD1b was also involved in the AGO4-dependent de novo DNA methylation pathway by subjecting the *nrpd1b* mutant to the same de novo methylation assay. Similar to *nrpd1a*, *nrpd1b* was unable to silence the *FWA* transgene, as indicated by a late-flowering phenotype when compared to wild-type (Figure 4A). This result suggests that both forms of Pol IV (NRPD1a and NRPD1b) are involved in AGO4-dependent de novo DNA methylation.

Because both *nrpd1a* and *nrpd1b* phenocopied *ago4-1* in the *FWA* transformation assay, it is possible that AGO4 might be functioning directly with Pol IV. To determine whether AGO4 is acting in concert with NRPD1a or

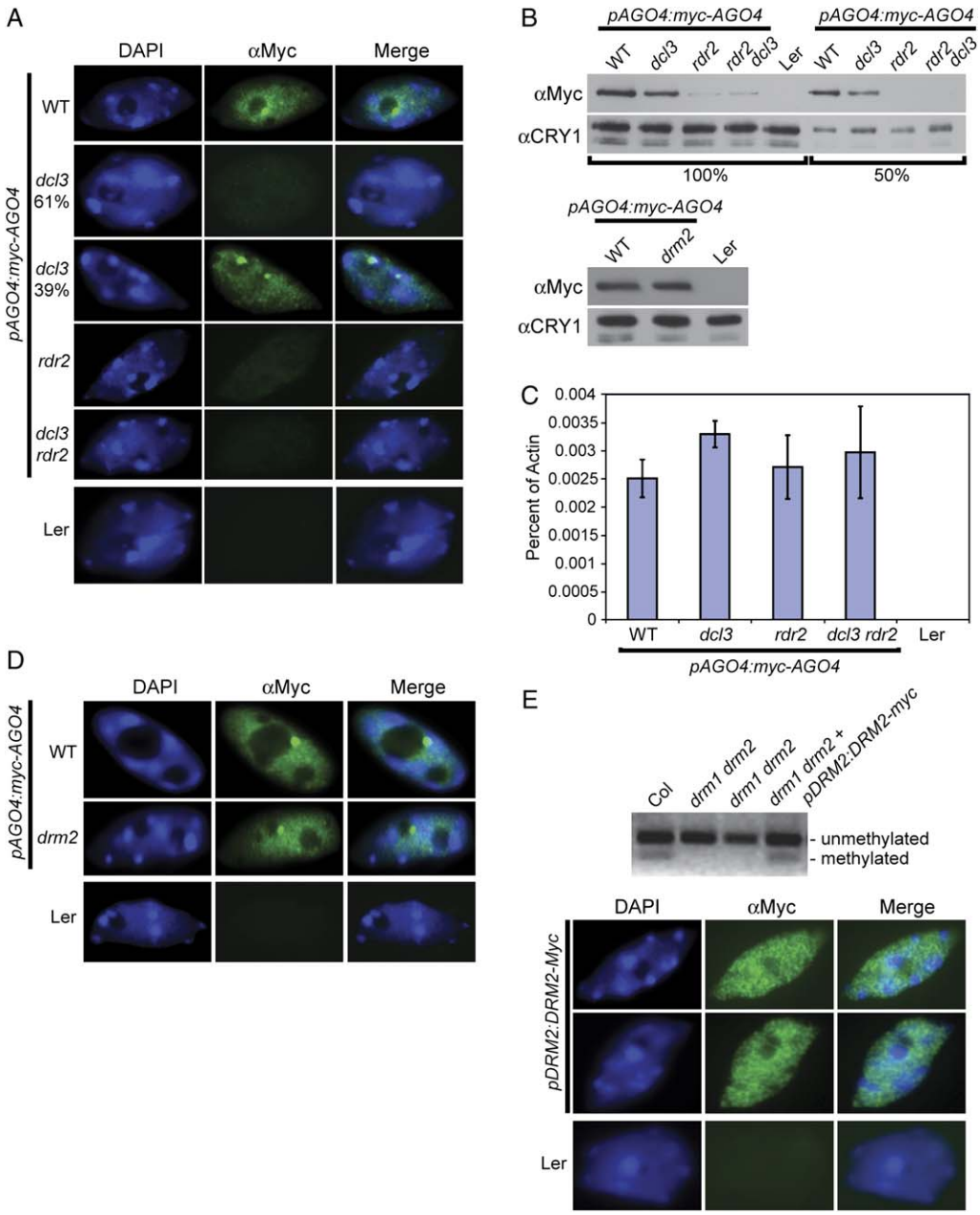

Figure 3. AGO4 Protein Levels Are Affected by the RNAi Mutants *rdr2* and *dcl3*

(A) Fluorescence microscopy analysis of Myc-AGO4 in wild-type, *dcl3*, *rdr2*, and *dcl3 rdr2* double mutants. Sixty-one percent of *dcl3* nuclei showed reduced Myc-AGO4 levels, while 39% showed wild-type levels (n = 70).

(B) Western blot analysis of Myc-AGO4 levels in various mutants. Protein extracts were normalized for total protein before loading. Half as much total protein was loaded for the 50% lanes. CRY1 was used as a loading control.

(C) Quantitative PCR analysis of *myc-AGO4* transcripts. *myc-AGO4* mRNA levels are expressed as a percentage of *ACTIN* transcript levels. The averages from two independent biological experiments with standard errors are shown.

(D) Fluorescence microscopy analysis of Myc-AGO4 localization in the DNA methyltransferase mutant *drm2*.

(E) Complementation and localization of DRM2-myc. Upper panel: *DRM2-myc* complements the *drm1 drm2* double mutant by the *MEA-ISR* bisulfite cutting assay. Lower panel: Fluorescence microscopy showing the localization of DRM2-myc in the nucleus.

NRPD1b, localization of NRPD1a or NRPD1b was examined in Myc-AGO4 nuclei using specific antibodies to NRPD1a or NRPD1b (Pontier et al., 2005). By fluorescence microscopy, NRPD1a did not colocalize with AGO4 (Figure 4B). Although NRPD1a showed localization to small speckles in the nucleus, none of these NRPD1a

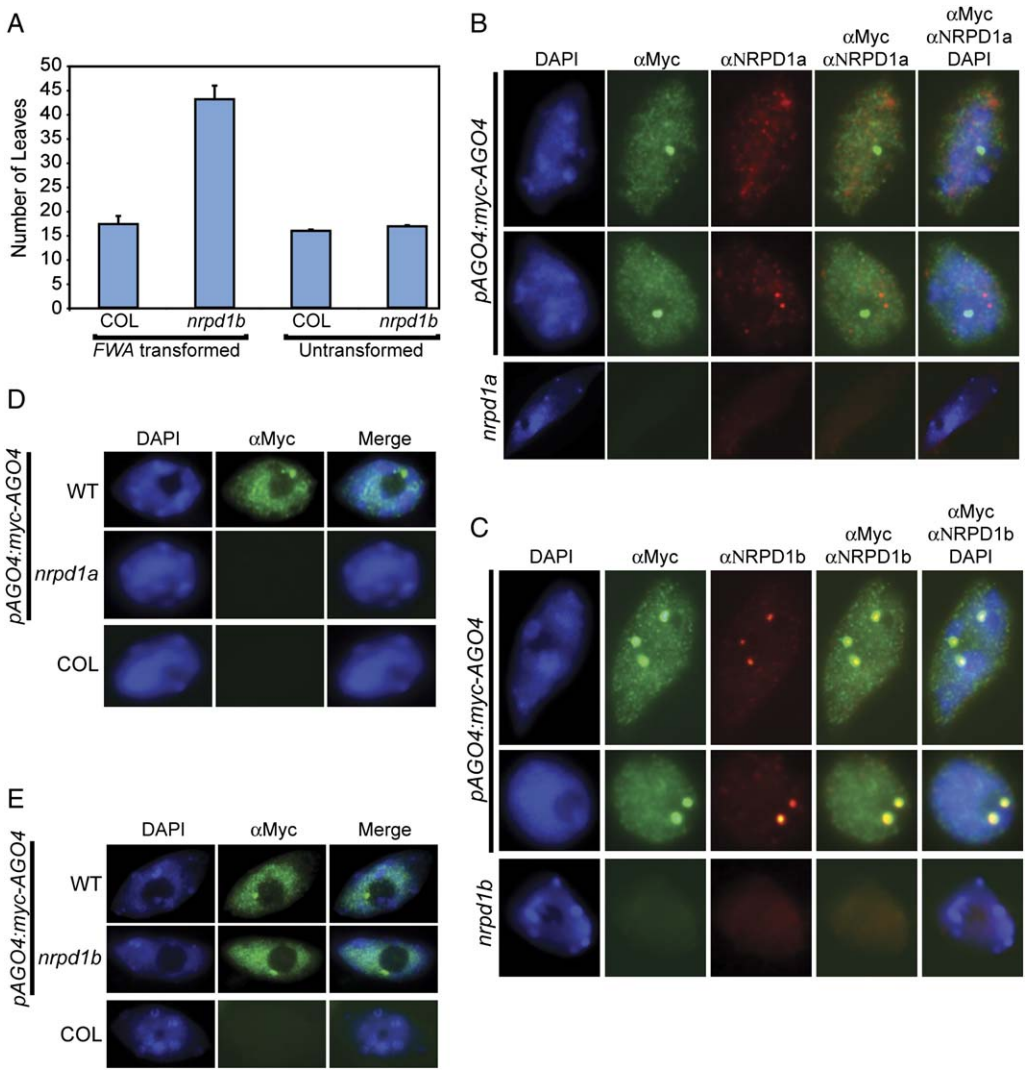

Figure 4. NRPD1b, but Not NRPD1a, Colocalizes with AGO4

(A) Flowering-time phenotype of the *nrpd1b* mutant transformed with *FWA*. First-generation transformants or their untransformed counterparts were scored for flowering time by the number of leaves. Standard errors for *FWA*-transformed Col (wild-type, n = 19) and *nrpd1b* (n = 12) or untransformed Col (n = 24) and *nrpd1b* (n = 27) are shown.

(B) Fluorescence microscopy analysis of NRPD1a localization relative to Myc-AGO4. A polyclonal antibody raised against NRPD1a was used for detecting endogenous protein.

(C) Colocalization of NRPD1b and AGO4 at the nuclear dot. NRPD1b localization was visualized by an anti-NRPD1b polyclonal antibody.

(D) Fluorescence microscopy analysis of Myc-AGO4 protein in the *nrpd1a* mutant.

(E) Fluorescence microscopy analysis of Myc-AGO4 protein in the *nrpd1b* mutant.

dots corresponded to the AGO4 body. In contrast, NRPD1b localized to the same nucleolar bodies as AGO4 did (Figure 4C; Table S1). This result demonstrates that the nucleolar body is not an AGO4-exclusive phenomenon and is relevant to other RNAi components involved in RNA-directed DNA methylation.

We also tested the effect of mutations in *NRPD1a* and *NRPD1b* on AGO4 localization. Similarly to *rdr2* and *dcl3* mutants, the Myc-AGO4 signal in nuclei was dramatically reduced in the *nrpd1a* mutant (Figure 4D). In contrast, *nrpd1b* had no effect on AGO4 nuclear localization patterns, either at the AGO4 body or outside of chromocenters (Figure 4E). Overall, these results are consistent with NRPD1a's acting upstream of AGO4 and NRPD1b's acting either at the same step or downstream of AGO4.

AGO4 Interacts with the C-Terminal Domain of NRPD1b

To determine whether AGO4 might form stable high-molecular-weight complexes with other proteins, we performed gel filtration chromatography with whole-cell lysates from Myc-AGO4 plants. We observed that, while

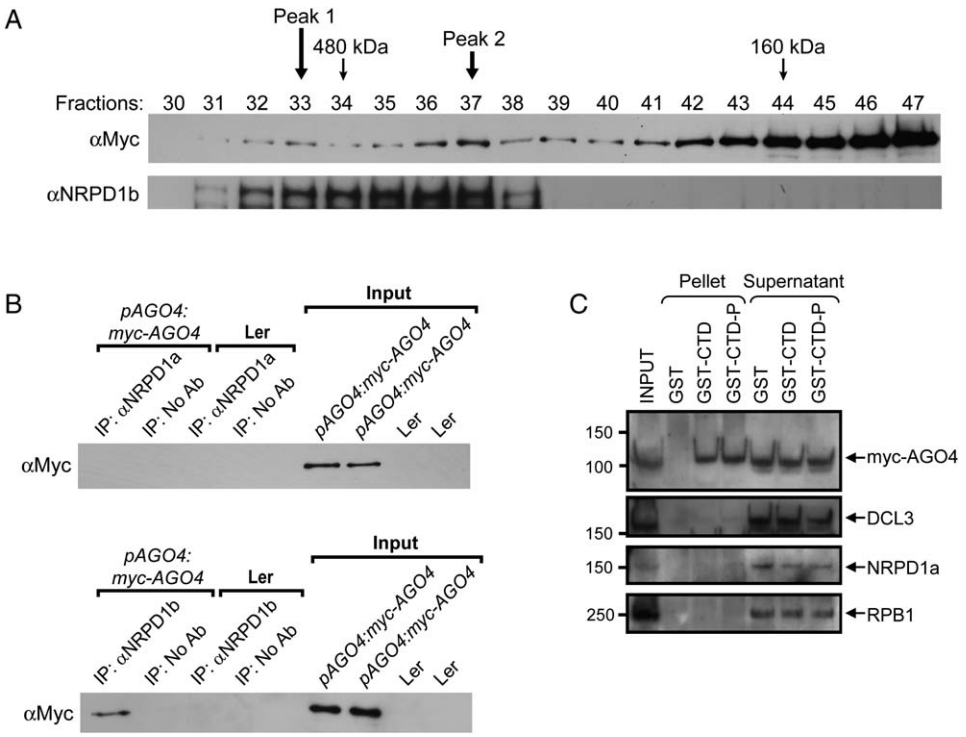

Figure 5. AGO4 Interacts with the CTD of NRPD1b

(A) Gel filtration analysis of Myc-AGO4 and NRPD1b. The two high-molecular-weight fraction peaks of Myc-AGO4 are indicated. The size of the second peak was estimated to be 280 kDa using a standard curve. The two smaller black arrows indicate fractions where the 480 kDa and 160 kDa protein standards eluted.

(B) Western blot analysis of the coimmunoprecipitation of Myc-AGO4 with NRPD1b but not with NRPD1a. NRPD1a (upper panel) or NRPD1b (lower panel) was immunoprecipitated from flower extracts containing Myc-AGO4 or no Myc-AGO4 (Ler), and copurified proteins were analyzed by SDS-PAGE followed by an anti-Myc Western blot analysis.

(C) AGO4 associates with the NRPD1b CTD domain. A whole-cell extract from Myc-AGO4 plants was applied onto GST, GST-CTD, or phosphorylated GST-CTD (GST-CTD-P) beads. After binding, the beads were pelleted and washed, and the bound proteins were detected by immunoblotting with anti-Myc, anti-DCL3, anti-NRPD1a, and anti-RPB1 antibodies. Input material (13% of total input), pellet fractions (30%), and supernatant fractions (13%) are shown. Molecular-weight sizes in kDa are noted on the left of the Western blots.

the majority of total AGO4 protein eluted at the size predicted for a monomer, a significant fraction of AGO4 was present in two high-molecular-weight complexes of around 280 kDa and greater than 480 kDa (Figure 5A). The colocalization of NRPD1b with Myc-AGO4 suggested the possibility that these proteins might interact. Consistent with this notion, we found that the elution profile of NRPD1b correlated with the high-molecular-weight AGO4 complexes (Figure 5A). To test whether NRPD1b and AGO4 are stably associated, we performed coimmunoprecipitation experiments. We found that antibodies specific for NRPD1b coprecipitated Myc-AGO4 (Figure 5B). Antibodies to NRPD1a, however, did not coprecipitate Myc-AGO4.

One structural difference between NRPD1a and NRPD1b is the presence of a large reiterated C-terminal domain (CTD) in NRPD1b (Pontier et al., 2005). A reiterated CTD (of different sequence) is also found in the largest subunit of RNA polymerase II (RPB1), where it serves as a binding site for other proteins, and its phosphorylation is involved in the transition of RNA polymerase II from a preinitiation state to elongation (Dahmus, 1996; Hampsey and Reinberg, 2003). We therefore tested whether AGO4 might interact with the NRPD1b CTD, in either its phosphorylated or unphosphorylated forms, by testing the ability of bacterially produced CTD-glutathione S-transferase fusion protein to capture Myc-AGO4 from crude protein extracts (Figure 5C). We found that AGO4, but not DCL3, NRPD1a, or RPB1, bound strongly to the NRPD1b CTD. In vitro phosphorylation of the GST-CTD neither enhanced nor inhibited binding to Myc-AGO4. These data, together with the coimmunoprecipitation and colocalization results, strongly suggest that AGO4 and NRPD1b interact with one another.

The AGO4 Nuclear Body Is Distinct from Major Sites of RNA-Directed DNA Methylation

AGO4 is involved in DNA methylation at the rDNA genes (Xie et al., 2004; C.S.P., unpublished data), and immunoprecipitated AGO4 contains 45S and 5S siRNAs, which also localize to the AGO4 body (see Pontes et al., 2006 in this issue of *Cell*). We therefore examined whether the

AGO4 nuclear body may represent a concentrated localization of AGO4 at the 45S or 5S rDNA loci. By DNA-FISH analysis, the AGO4 body did not colocalize with the nucleolar organizer regions (NORs), which contain the 45S rDNA genes, or with the 5S rDNA genes (Figure 2B; Table S2) (Grummt and Pikaard, 2003). These findings suggest that the AGO4 body is likely not a major site of RNA-directed DNA methylation at AGO4 target loci, which is also consistent with the fact that DRM2 is not enriched at the AGO4 body.

A Homolog of the Small Nuclear RNA Binding Protein SmD3 Is Found at the AGO4 Nuclear Body

To learn more about the nature of the AGO4 nuclear body, we searched for proteins that display the same subnuclear localization as AGO4. A recent study showed localization of a large number of nucleolar-associated proteins in *Arabidopsis* (Pendle et al., 2005). Several of these proteins, including an *Arabidopsis* homolog of the small nuclear RNA (snRNA) binding protein SmD3, displayed localization to a body in or near the nucleolus (Pendle et al., 2005). SmD3 is a core protein component of the U1, U2, U4, and U5 small nuclear ribonucleoproteins (snRNPs), which are central components of the spliceosome (Khusial et al., 2005). We transformed Myc-AGO4 plants with GFP-SmD3 (Pendle et al., 2005) and generated a stable line expressing both fusion proteins. We observed a nearly perfect colocalization of GFP-SmD3 and Myc-AGO4, both predominantly labeling a nucleolar or perinucleolar body (Figure 6A; Table S1).

AGO4 Nuclear Bodies Correspond to Cajal Bodies

The Cajal body is a well-studied nuclear compartment that is involved in the processing and maturation of several types of ribonucleoprotein complexes (Cioce and Lamond, 2005; Shaw and Brown, 2004). For instance, snRNPs are posttranscriptionally modified and associate with specific proteins in the Cajal body before leaving the Cajal body to participate in splicing (Cioce and Lamond, 2005). Because of the localization of AGO4 with SmD3 (a putative component of snRNPs), we hypothesized that the AGO4 body might be a Cajal body. This hypothesis was supported by our finding that the AGO4 body stained poorly with DAPI (Cajal bodies contain little DNA [Boudonck et al., 1999]) and by previous work showing that Cajal bodies in *Arabidopsis* and many other plants are often associated with nucleoli (either perinucleolar or within nucleoli) (Beven et al., 1995; Boudonck et al., 1998, 1999; Chamberland and Lafontaine, 1993; Shaw and Brown, 2004).

We utilized two antibodies that recognize reliable markers of plant Cajal bodies, the 5′ 2,2,7-trimethylguanosine (TMG) cap of snRNAs and the U2-specific snRNA binding protein U2B″. snRNAs are TMG modified in the cytoplasm and are then imported to the nucleus, where they temporarily accumulate in Cajal bodies (Cioce and Lamond, 2005; Mattaj, 1986). TMG caps are found on *Arabidopsis* snRNAs (Lorkovic et al., 2004; Vankan and Filipowicz, 1988), and TMG-capped snRNAs are markers of Cajal bodies in *Arabidopsis* and other plant species (Chamberland and Lafontaine, 1993; Docquier et al., 2004). The U2B″ protein specifically associates with *Arabidopsis* TMG-capped U2 snRNA (Lorkovic et al., 2004) and colocalizes with TMG-capped snRNAs and with the core snRNA binding protein SmB at *Arabidopsis* Cajal bodies (Docquier et al., 2004; Lorkovic et al., 2004). U2B″ has been used in studies of the behavior of Cajal bodies in *Arabidopsis* and other plants (Boudonck et al., 1998, 1999; Docquier et al., 2004) and colocalizes in *Arabidopsis* with an antibody recognizing coilin, a protein specifically found in Cajal bodies (Beven et al., 1995).

We tested whether AGO4 and SmD3 colocalize with these Cajal body markers. Nuclei from GFP-SmD3 plants were stained with monoclonal antibodies against TMG and U2B″ (Figures 6B and 6C). We observed a nearly perfect colocalization of GFP fluorescence with both TMG-capped snRNAs and U2B″ (Table S1). To examine the colocalization of Myc-AGO4 with Cajal body markers, we utilized a Myc polyclonal antibody together with monoclonal TMG and U2B″ antibodies (Figures 6D and 6E). Although the polyclonal Myc antibody gave a somewhat higher background than the monoclonal Myc antibody used throughout the rest of this study, the AGO4 nuclear body was still clearly evident. We observed a nearly perfect colocalization of Myc-AGO4 with both the TMG snRNAs and U2B″ signals (Figures 6D and 6E; Table S1). These findings strongly suggest that AGO4 bodies correspond to Cajal bodies.

To determine whether upstream RNA silencing mutants affect the integrity of Cajal bodies, we tested the localization of TMG snRNAs and U2B″ in the *nrpd1a* and *rdr2* mutants. Neither mutant showed reduced staining of Cajal body markers (Figure S1). Thus, while these mutants eliminate AGO4 association with Cajal bodies, they do not disrupt the basic integrity of the Cajal body or the localization of snRNAs or U2B″.

DISCUSSION

The instability of AGO4 in certain RNAi silencing mutants allows us to determine an order of action of some of the proteins involved in RdDM. The observation that AGO4 is destabilized in the *nrpd1a*, *rdr2*, and *dcl3* mutants could be explained by either a physical interaction between these proteins with AGO4 or the fact that these proteins synthesize siRNAs for incorporation into AGO4. Since our data suggest that AGO4 did not associate or colocalize with NRPD1a and since our gel filtration results showed that the majority of AGO4 protein exists as a monomer, we strongly favor the latter hypothesis—that, in the absence of 24 nucleotide siRNAs synthesized by NRPD1a, RDR2, and DCL3, the AGO4 protein becomes unstable. This interpretation also fits with our observations that AGO4 immunoprecipitates 24 nucleotide siRNAs and that siRNAs colocalize with AGO4 within the nucleolar bodies (Pontes et al., 2006). This may represent a requirement of siRNAs for the basic structural integrity of

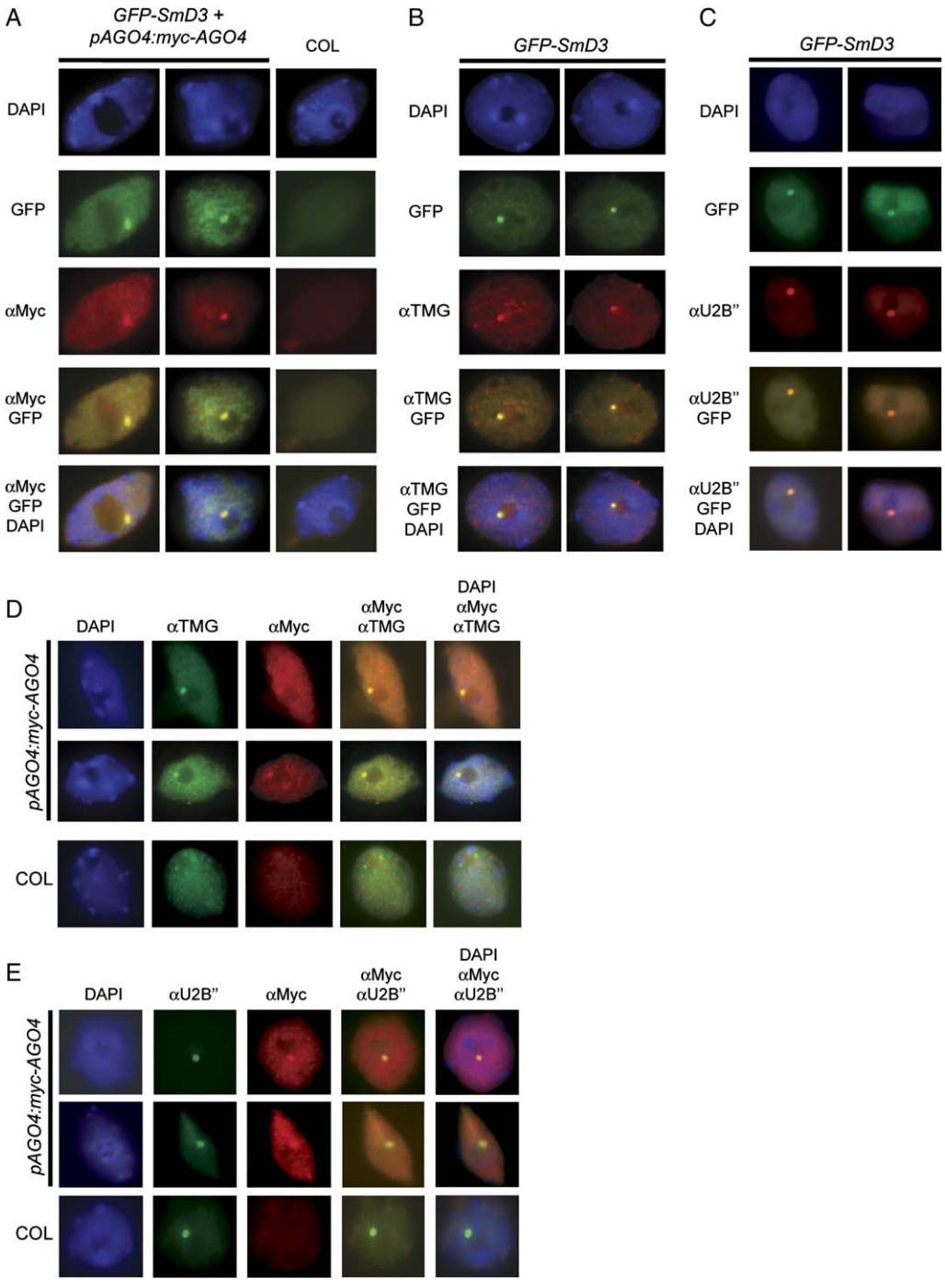

Figure 6. The AGO4 Body Colocalizes with SmD3 and Cajal Body Markers

(A) GFP-SmD3 colocalizes with Myc-AGO4 in transgenic *GFP-SmD3 myc-AGO4* plants.

(B) GFP-SmD3 colocalizes with TMG-capped snRNAs in *GFP-SmD3* nuclei.

(C) GFP-SmD3 colocalizes with U2B″ in *GFP-SmD3* nuclei.

(D) Myc-AGO4 colocalizes with TMG-capped snRNAs in *myc-AGO4* nuclei. A polyclonal anti-Myc antibody was used to detect Myc-AGO4.

(E) Myc-AGO4 colocalizes with U2B″ in *myc-AGO4* nuclei. Myc-AGO4 was detected using polyclonal Myc antibody.

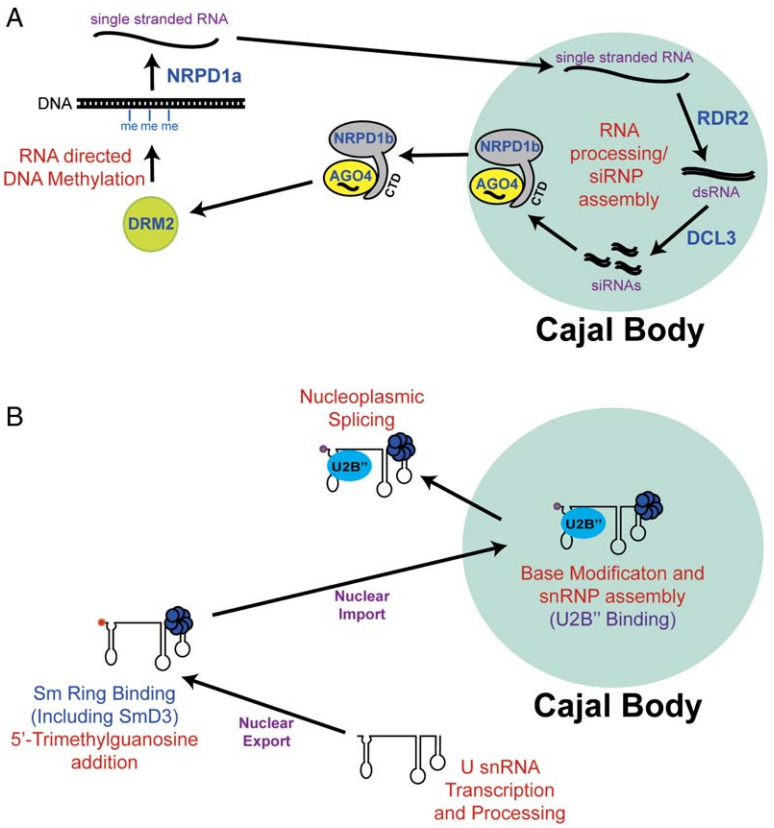

Figure 7. Comparison of siRNP and snRNP Processes Associated with Cajal Bodies

(A) Model for the localization and functioning of components of the 24 nucleotide siRNA RNA-directed DNA methylation pathway and their association with Cajal bodies. Single-stranded NRPD1a-produced RNAs from overexpressed transgenes, transposable elements, or other repetitive loci localize to Cajal bodies, where they are processed into double-stranded RNA (dsRNA) and siRNAs by RDR2 and DCL3. siRNAs are incorporated into an AGO4/NRPD1b complex (siRNA protein complex; siRNP). This AGO4/NRPD1b/siRNA complex then relocates to target loci and activates DRM2 to cause RdDM and transcriptional gene silencing. DNA methylation or other associated chromatin modifications stimulate the production of RNA competent for further rounds of siRNA production.

(B) Analogy of RNA-directed DNA methylation processes to the maturation of snRNPs in Cajal bodies. snRNAs are transcribed in the nucleus and then exported to the cytoplasm, where they associate with a heptameric ring of core Sm proteins (including SmD3). These snRNPs are reimported into the nucleus, where they concentrate in Cajal bodies, become posttranscriptionally modified, and associate with specific proteins (such as U2B″ in the case of the U2 snRNA). Mature snRNPs leave the Cajal body to function in splicing in the nucleoplasm.

AGO4 or a more complex regulated phenomenon that ensures the proper channeling of particular siRNAs into AGO4 from the appropriate pathways, thus preventing the promiscuous utilization of irrelevant small RNAs.

Regardless of the particular mechanisms involved, these results clearly place the action of NRPD1a, RDR2, and DCL3 upstream of the action of AGO4 (Figure 7A). Conversely, our finding that the *nrpd1b* and *drm2* mutants do not alter the pattern of AGO4 accumulation suggests that these factors act either downstream of or at the same step as AGO4. This order of action is supported by data showing that the *nrpd1a*, *rdr2*, and *dcl3* mutants strongly reduce siRNA accumulation at the majority of endogenous loci, while the *ago4*, *nrpd1b*, and *drm2* mutants show more minor and locus-specific effects, which may involve a feedback between DNA methylation and siRNA production (Kanno et al., 2005; Pontes et al., 2006; Pontier et al., 2005; Xie et al., 2004; Zilberman et al., 2004) (Figure 7A).

Our finding that NRPD1b interacts with AGO4 through its C-terminal domain is further evidence for the important roles that NRPD1b and AGO4 play in the downstream targeting of DNA methylation, after siRNAs have been generated by NRPD1a, RDR2, and DCL3. One possibility is that NRPD1b synthesizes a nascent RNA transcript from DNA methylated loci and that this transcript acts as a binding site for a siRNA bound AGO4 molecule. The physical association of NRPD1b and AGO4 might ensure efficient coupling of these two events.

Remarkably, we found that AGO4 and NRPD1b localize to a nuclear body either within or adjacent to the nucleolus. This body is not a chromocenter since it does not stain with the DNA stain DAPI, does not contain centromeric DNA sequences, and does not contain detectable levels of histones dimethylated at lysine 9. Furthermore, this body does not appear to be a major site of RNA-directed DNA methylation since it does not contain detectable levels of DNA for two major AGO4 target sites, the 45S and 5S rDNAs, and does not contain the DRM2 DNA methyltransferase. Instead, we found that the AGO4 body colocalizes with a plant homolog of one of the core snRNA binding proteins, SmD3, and also with two markers of Cajal bodies, TMG-capped snRNAs and the U2-specific binding protein U2B″, strongly suggesting that AGO4 localizes to Cajal bodies.

Cajal bodies were originally discovered more than 100 years ago by Santiago Ramon y Cajal in vertebrate neurons and have subsequently been studied in a variety of animal and plant systems (Gall, 2003). They are multifunctional centers for the recycling and maturation of snRNPs, the trafficking of telomerase RNA (also associated with SmD3; Fu and Collins, 2006), biogenesis of small nucleolar RNPs (snoRNPs), histone mRNA 3′ end processing, and posttranscriptional modification (2′-O-methylation and pseudouridylation) of snRNAs by small Cajal body-specific RNAs (scaRNAs) (Cioce and Lamond, 2005; Shaw and Brown, 2004).

The finding that AGO4 colocalizes with Cajal bodies, together with the observation that AGO4 and NRPD1b colocalize with DCL3, RDR2, and siRNAs in these bodies (Pontes et al., 2006), suggests that several components of the 24 nucleotide siRNA transcriptional silencing pathway may function within Cajal bodies. However, two important components of this pathway, NRPD1a and DRM2, are not concentrated in Cajal bodies. Based on these results, we propose a model for how AGO4/Cajal bodies may couple RNA processing events with the loading of siRNAs into an AGO4/NRPD1b complex for use in RNA-directed DNA methylation (Figure 7A). In this model, NRPD1a acts at an upstream step in the process to synthesize single-stranded RNA from transposons, highly repetitive loci, overexpressed transgenes, or viruses that are subject to RNA-directed DNA methylation (Pontes et al., 2006; Wassenegger, 2005). NRPD1a-produced RNAs would then be recruited by an unknown mechanism to Cajal bodies, where they would be processed by RDR2, which converts the single-stranded RNA to double-stranded RNA, and DCL3, which dices the double-stranded RNA into 24 nucleotide siRNAs. These siRNAs would be loaded into an AGO4/NRPD1b complex that would then leave the Cajal body and activate the DRM2 methyltransferase to cause RdDM at corresponding DNAs. Chromatin modifications at target loci might then serve to reinforce further recruitment of RNAi machinery components (possibly through the activity of NRPD1b) to maintain further rounds of siRNA-mediated silencing, which is supported by the finding that DRM2 is required for the maintenance of siRNAs at some target loci (Xie et al., 2004; Zilberman et al., 2004).

The finding that key components of the RdDM pathway are concentrated in Cajal bodies has parallels with the discovery that miRNA-mediated posttranscriptional silencing is associated with the localization of microRNAs and AGO proteins to cytoplasmic processing bodies (P bodies) (Jabri, 2005). The sequestering or concentrating of important events related to the RdDM pathway (such as the dicing of RNAs and the loading of AGO4) to Cajal bodies may prevent illegitimate events from occurring elsewhere, thereby increasing the fidelity of silencing pathways. Given the precedent for RNA modification in Cajal bodies, it is also possible that siRNAs are methylated or uridylated in this compartment (Li et al., 2005).

Cajal bodies are dynamic structures, fusing to one another and moving within nuclei and nucleoli, and Cajal body-associated molecules are known to move rapidly in and out of Cajal bodies (Shaw and Brown, 2004). Thus, the flux of components of the 24 nucleotide silencing pathway such as AGO4, NRPD1b, DCL3, and RDR2 through Cajal bodies could play a critical role in the processes regulating RNA-directed DNA methylation. Our model for the processing and loading of siRNAs into AGO4/NRPD1b within the Cajal body and its functioning in RNA-directed DNA methylation at sites distant from the Cajal body has many parallels with the biogenesis of snRNPs, which is accompanied by intracellular trafficking though Cajal bodies where the snRNPs are modified and associated with snRNA-specific proteins (see model in Figure 7B) (Cioce and Lamond, 2005; Shaw and Brown, 2004). Our data suggest a function for plant Cajal bodies in the generation of siRNA/protein complexes that act in RNA-directed DNA methylation.

EXPERIMENTAL PROCEDURES

Generation of Epitope-Tagged Lines

AGO4 containing 3.7 kb of endogenous promoter was amplified from BAC clone T20P8 and subcloned into pCAMBIA1300a. ApaI and BamHI restriction sites were engineered immediately upstream of the AGO4 start codon, and four copies of c-Myc were inserted in-frame. *Agrobacterium* strain ASE was used to transform *ago4-1 clk-st* plants using hygromycin selection (Bechtold and Pelletier, 1998). Several lines were analyzed by Western blot and immunofluorescence, and all showed similar levels of Myc-AGO4 expression, suggesting that genomic position effects were minimal.

The *DRM2* gene and flanking intergenic regions were amplified from BAC clone T15N1, cloned into pCR4 (Invitrogen), and sequenced. NheI and BamHI sites were introduced by site-directed mutagenesis, and a 9× Myc epitope was inserted just before the DRM2 stop codon. Myc-tagged *DRM2* was then cloned into the pCAMBIA1300 and transformed, selected, and analyzed as above.

The plasmid containing GFP-SmD3 was a gift from Peter J. Shaw (Pendle et al., 2005) and was transformed using *Agrobacterium* strain AGL1.

Loss-of-Function Mutants

The mutants used in this study were previously described: *dcl3-1* and *rdr2-1* (Xie et al., 2004), *drm2* (Cao and Jacobsen, 2002), and *nrpd1b-1* and *nrpd1b-2* (Pontier et al., 2005). The T-DNA mutant *nrpd1a* (SALK 143437) was obtained from the Arabidopsis Biological Resource Center.

MEA-ISR Cutting Assay

Genomic DNA was digested with FokI and subjected to sodium bisulfite treatment as described (Jacobsen et al., 2000). *MEA-ISR* was amplified by PCR using primers 5′-AAAGTGGTTGTAGTTTATGAAAGGTTTTAT-3′ and 5′-CTTAAAAAATTTTCAACTCATTTTTAAAAAA-3′. PCR products were digested with BamHI and resolved by agarose gel electrophoresis. Presence of a full-length (~360 bp) or digested (~270 bp) PCR product indicated the absence or presence of DNA methylation, respectively.

Immunofluorescence Analysis

Preparation of nuclei without flow sorting was performed as described (Jasencakova et al., 2003). Primary antibodies used included mAb Myc (1:200, Upstate), polyclonal Myc (1:100, Upstate), H3K9me2 (1:200, Upstate), H3K27me3 (1:400, Upstate), NRPD1a (1:200), NRPD1b (1:100), mAb 4G3 (anti-U2B″) (1:100, gift from Gregory Matera), and mAb K-121 (anti-TMG cap) (1:100, Calbiochem). Secondary anti-mouse fluorescein (Abcam), anti-rabbit rhodamine (Jackson ImmunoResearch), anti-mouse rhodamine (Abcam), anti-mouse Alexa Fluor 488 (Invitrogen), anti-mouse FITC (Abcam), and anti-rabbit Alexa Fluor 555 (Invitrogen) were used at 1:200 dilution. Vectashield mounting medium containing DAPI (Vector Laboratories) was added to nuclei to visualize DNA and prevent fading. Nuclear protein localization was captured at 100× magnification using the Zeiss Axioskop 2 microscope with the Zeiss Axiocam HRC color digital camera system or the Zeiss AxioImager Z1 microscope with the Hamamatsu Orca-ER camera. Images were analyzed using Zeiss AxioVision software and processed using Adobe Photoshop (Adobe Systems).

Quantitative RT-PCR Analysis

RNA was isolated and cDNA was generated as previously described (Johnson et al., 2002). Real-time PCR amplification was performed using SYBR Green QPCR Master Mix (Stratagene). Data were analyzed using the Mx3000P software (Stratagene).

Western Blot Analysis

Flowers (0.3 g) were frozen in liquid nitrogen; ground into powder; homogenized with 1 ml of protein extraction buffer (50 mM Tris-Cl [pH 7.5], 150 mM NaCl, 5 mM $MgCl_2$, 10% glycerol, 0.1% NP-40) containing fresh DTT (2 mM), PMSF (1 mM), pepstatin (0.7 μg/ml), MG132 (10 μg/ml), and protease inhibitor cocktail (Roche); and centrifuged twice (13,000 rpm at 4°C). Equal total protein amounts were resolved on an 8% SDS polyacrylamide gel and subjected to Western blotting using a Myc monoclonal antibody (Upstate).

Coimmunoprecipitation of AGO4 and RNA Pol IV

Cell lysates were prepared as described in the previous section using 0.7 g of flowers and 2 ml of protein extraction buffer. Equal total protein amounts were precleared with Protein A agarose beads (Pierce), followed by anti-NRPD1a or anti-NRPD1b incubation (1:250). Protein complexes were captured with Protein A agarose beads, washed five times with extraction buffer, boiled in SDS sample buffer, resolved on an 8% SDS polyacrylamide gel, and subjected to Western blotting.

Gel Filtration Analysis of Myc-AGO4

Myc-AGO4 lysates from flowers were prepared as described in the previous section. The lysates were additionally filtered through a 0.2 μm filter. Four milligrams of total protein was loaded onto a Superdex 200 10/300 GL column (Amersham), and 250 μl fractions were collected at 0.5 ml/min. To determine complex sizes, a standard curve was generated using the calibration proteins apoferritin (480 kDa), γ-globulin (160 kDa), bovine serum albumin (67 kDa), chymotrypsinogen (24 kDa), and cytochrome c (13 kDa).

GST-CTD Binding Experiments

The NRPD1b CTD (from amino acid 1410 to 1874) was amplified from reverse-transcribed cDNA, cloned into the overexpression plasmid pET-41a(+) (Novagen), and expressed in *E. coli* BL21. Expression was induced for 3 hr with 1 mM IPTG in cells grown at 37°C to an OD_{600} of 0.6. Cells were disrupted using a French press, and the GST-fusion proteins were purified by glutathione Sepharose 4B (Amersham Biosciences) affinity chromatography. The GST-CTD fusion protein was in vitro phosphorylated using casein kinase (New England Biolabs) as previously described for the RNA Pol II-derived GST-CTD fusion protein (Barilla et al., 2001). Phosphorylation of the CTD was confirmed by electrophoresis in an SDS-polyacrylamide gel in which the phosphorylated form is indicated by its retarded mobility. Unphosphorylated and phosphorylated GST-CTD and GST proteins were immobilized onto 20 μl of glutathione Sepharose 4B, and the coated beads were washed and equilibrated with IP buffer. A total of 150 μl of flower whole-cell extract was applied to the GST-CTD beads and mixed for 3 hr at 4°C on a rotating wheel. The beads were then washed three times with IP buffer, and the bound protein (pellet) was eluted with 60 μl of SDS-PAGE sample buffer. All samples including the unbound proteins (supernatant) were separated by 10% SDS-PAGE and subjected to Western blotting.

DNA-FISH Analysis

DNA-FISH using 5S or 45S rRNA gene probes labeled with biotin-dUTP or digoxigenin-dUTP was performed as described (Pontes et al., 2003). Digoxigenin-labeled probes were detected using mouse anti-digoxigenin antibody (1:250, Roche) followed by rabbit anti-mouse antibody conjugated to Alexa 488 (Molecular Probes). Biotin-labeled probes were detected using goat anti-biotin conjugated with avidin (1:200, Vector Laboratories) followed by streptavidin-Alexa 543 (Molecular Probes). DNA was counterstained with DAPI (1 μg/ml) in Vectashield. For dual protein/nucleic-acid localization experiments, slides were first subjected to immunofluorescence and then postfixed in 4% formaldehyde/PBS followed by DNA-FISH. Nuclei were examined using a Nikon Eclipse E80i epifluorescence microscope, with images collected using a Photometrics Coolsnap ES Mono digital camera. The images were pseudocolored, merged, and processed using Adobe Photoshop (Adobe Systems).

Supplemental Data

Supplemental Data include one figure and three tables and can be found with this article online at http://www.cell.com/cgi/content/full/126/1/93/DC1/.

ACKNOWLEDGMENTS

We thank Utpal Banerjee for use of a fluorescence microscope; Lianna Johnson for microscopy training; Ingo Schubert for nuclear staining protocols and advice; Peter Shaw for plasmids; Greg Matera, Doug Black, and Chentao Lin for antibodies; Feng Guo for the use of his chromatography system; Michael Faller for chromatography training; Van Dinh for technical assistance; and Doug Black, Peter Shaw, and Angus Lamond for useful discussions. O.P. performed DNA-FISH experiments. T.L. provided polyclonal NRPD1a and NRPD1b antibodies. M.E.-S. performed GST-CTD pull-down experiments. Generation, complementation, and immunofluorescence analysis of DRM2-myc were performed by I.R.H. S.W.-L.C. performed flowering-time experiments. Y.V.B. performed TMG and U2B″ immunofluorescence experiments. C.F.L. performed all other experiments, and C.F.L. and S.E.J. wrote the manuscript. C.F.L. was supported by the Ruth L. Kirschstein National Research Service Award GM07185, and Y.V.B. was supported by USPHS National Research Service Award GM07104. I.R.H. was supported by an EMBO long-term fellowship. S.W.-L.C. is a DOE Energy Biosciences fellow of the Life Science Research Foundation. T.L. was supported by Génoplante grant GEN-061 and ANR grant NT05-3_45717. Pikaard lab work was supported by NIH grants R01GM60380 and R01GM077590. O.P. was supported by fellowship SFRH/BPD/17508/2004 from the Fundação para a Ciência e Tecnologia (Portugal). S.E.J. is an investigator of the Howard Hughes Medical Institute. Jacobsen lab research was supported by NIH grant GM60398.

Received: March 2, 2006
Revised: April 7, 2006
Accepted: May 17, 2006
Published: July 13, 2006

REFERENCES

Barilla, D., Lee, B.A., and Proudfoot, N.J. (2001). Cleavage/polyadenylation factor IA associates with the carboxyl-terminal domain of RNA polymerase II in Saccharomyces cerevisiae. Proc. Natl. Acad. Sci. USA *98*, 445–450.

Bechtold, N., and Pelletier, G. (1998). In planta Agrobacterium-mediated transformation of adult Arabidopsis thaliana plants by vacuum infiltration. Methods Mol. Biol. *82*, 259–266.

Beven, A.F., Simpson, G.G., Brown, J.W., and Shaw, P.J. (1995). The organization of spliceosomal components in the nuclei of higher plants. J. Cell Sci. *108*, 509–518.

Boudonck, K., Dolan, L., and Shaw, P.J. (1998). Coiled body numbers in the Arabidopsis root epidermis are regulated by cell type, developmental stage and cell cycle parameters. J. Cell Sci. *111*, 3687–3694.

Boudonck, K., Dolan, L., and Shaw, P.J. (1999). The movement of coiled bodies visualized in living plant cells by the green fluorescent protein. Mol. Biol. Cell *10*, 2297–2307.

Cao, X., and Jacobsen, S.E. (2002). Role of the Arabidopsis DRM methyltransferases in *de novo* DNA methylation and gene silencing. Curr. Biol. *12*, 1138–1144.

Carmell, M.A., Xuan, Z., Zhang, M.Q., and Hannon, G.J. (2002). The Argonaute family: tentacles that reach into RNAi, developmental control, stem cell maintenance, and tumorigenesis. Genes Dev. *16*, 2733–2742.

Chamberland, H., and Lafontaine, J.G. (1993). Localization of snRNP antigens in nucleolus-associated bodies: study of plant interphase nuclei by confocal and electron microscopy. Chromosoma *102*, 220–226.

Chan, S.W., Zilberman, D., Xie, Z., Johansen, L.K., Carrington, J.C., and Jacobsen, S.E. (2004). RNA silencing genes control de novo DNA methylation. Science *303*, 1336.

Chan, S.W., Henderson, I.R., and Jacobsen, S.E. (2005). Gardening the genome: DNA methylation in Arabidopsis thaliana. Nat. Rev. Genet. *6*, 351–360.

Chanvivattana, Y., Bishopp, A., Schubert, D., Stock, C., Moon, Y.H., Sung, Z.R., and Goodrich, J. (2004). Interaction of Polycomb-group proteins controlling flowering in Arabidopsis. Development *131*, 5263–5276.

Cioce, M., and Lamond, A.I. (2005). Cajal bodies: a long history of discovery. Annu. Rev. Cell Dev. Biol. *21*, 105–131.

Dahmus, M.E. (1996). Reversible phosphorylation of the C-terminal domain of RNA polymerase II. J. Biol. Chem. *271*, 19009–19012.

Docquier, S., Tillemans, V., Deltour, R., and Motte, P. (2004). Nuclear bodies and compartmentalization of pre-mRNA splicing factors in higher plants. Chromosoma *112*, 255–266.

Fagard, M., Boutet, S., Morel, J.B., Bellini, C., and Vaucheret, H. (2000). AGO1, QDE-2, and RDE-1 are related proteins required for post- transcriptional gene silencing in plants, quelling in fungi, and RNA interference in animals. Proc. Natl. Acad. Sci. USA *97*, 11650–11654.

Fransz, P., De Jong, J.H., Lysak, M., Castiglione, M.R., and Schubert, I. (2002). Interphase chromosomes in Arabidopsis are organized as well defined chromocenters from which euchromatin loops emanate. Proc. Natl. Acad. Sci. USA *99*, 14584–14589.

Fu, D., and Collins, K. (2006). Human telomerase and Cajal body ribonucleoproteins share a unique specificity of Sm protein association. Genes Dev. *20*, 531–536.

Gall, J.G. (2003). The centennial of the Cajal body. Nat. Rev. Mol. Cell Biol. *4*, 975–980.

Grummt, I., and Pikaard, C.S. (2003). Epigenetic silencing of RNA polymerase I transcription. Nat. Rev. Mol. Cell Biol. *4*, 641–649.

Hampsey, M., and Reinberg, D. (2003). Tails of intrigue: phosphorylation of RNA polymerase II mediates histone methylation. Cell *113*, 429–432.

Hannon, G.J. (2002). RNA interference. Nature *418*, 244–251.

Herr, A.J., Jensen, M.B., Dalmay, T., and Baulcombe, D.C. (2005). RNA polymerase IV directs silencing of endogenous DNA. Science *308*, 118–120.

Jabri, E. (2005). P-bodies take a RISC. Nat. Struct. Mol. Biol. *12*, 564.

Jacobsen, S.E., and Meyerowitz, E.M. (1997). Hypermethylated *SUPERMAN* epigenetic alleles in arabidopsis. Science *277*, 1100–1103.

Jacobsen, S.E., Sakai, H., Finnegan, E.J., Cao, X., and Meyerowitz, E.M. (2000). Ectopic hypermethylation of flower-specific genes in Arabidopsis. Curr. Biol. *10*, 179–186.

Jasencakova, Z., Soppe, W.J., Meister, A., Gernand, D., Turner, B.M., and Schubert, I. (2003). Histone modifications in Arabidopsis- high methylation of H3 lysine 9 is dispensable for constitutive heterochromatin. Plant J. *33*, 471–480.

Johnson, L., Cao, X., and Jacobsen, S. (2002). Interplay between two epigenetic marks. DNA methylation and histone H3 lysine 9 methylation. Curr. Biol. *12*, 1360–1367.

Kanno, T., Huettel, B., Mette, M.F., Aufsatz, W., Jaligot, E., Daxinger, L., Kreil, D.P., Matzke, M., and Matzke, A.J. (2005). Atypical RNA polymerase subunits required for RNA-directed DNA methylation. Nat. Genet. *37*, 761–765.

Khusial, P., Plaag, R., and Zieve, G.W. (2005). LSm proteins form heptameric rings that bind to RNA via repeating motifs. Trends Biochem. Sci. *30*, 522–528.

Li, J., Yang, Z., Yu, B., Liu, J., and Chen, X. (2005). Methylation protects miRNAs and siRNAs from a 3′-end uridylation activity in Arabidopsis. Curr. Biol. *15*, 1501–1507.

Lin, C., Ahmad, M., and Cashmore, A.R. (1996). Arabidopsis cryptochrome 1 is a soluble protein mediating blue light-dependent regulation of plant growth and development. Plant J. *10*, 893–902.

Lindroth, A.M., Shultis, D., Jasencakova, Z., Fuchs, J., Johnson, L., Schubert, D., Patnaik, D., Pradhan, S., Goodrich, J., Schubert, I., et al. (2004). Dual histone H3 methylation marks at lysines 9 and 27 required for interaction with CHROMOMETHYLASE3. EMBO J. *23*, 4286–4296.

Lorkovic, Z.J., Hilscher, J., and Barta, A. (2004). Use of fluorescent protein tags to study nuclear organization of the spliceosomal machinery in transiently transformed living plant cells. Mol. Biol. Cell *15*, 3233–3243.

Mathieu, O., Probst, A.V., and Paszkowski, J. (2005). Distinct regulation of histone H3 methylation at lysines 27 and 9 by CpG methylation in Arabidopsis. EMBO J. *24*, 2783–2791.

Mattaj, I.W. (1986). Cap trimethylation of U snRNA is cytoplasmic and dependent on U snRNP protein binding. Cell *46*, 905–911.

Meister, G., and Tuschl, T. (2004). Mechanisms of gene silencing by double-stranded RNA. Nature *431*, 343–349.

Onodera, Y., Haag, J.R., Ream, T., Nunes, P.C., Pontes, O., and Pikaard, C.S. (2005). Plant nuclear RNA polymerase IV mediates siRNA and DNA methylation-dependent heterochromatin formation. Cell *120*, 613–622.

Pendle, A.F., Clark, G.P., Boon, R., Lewandowska, D., Lam, Y.W., Andersen, J., Mann, M., Lamond, A.I., Brown, J.W., and Shaw, P.J. (2005). Proteomic analysis of the Arabidopsis nucleolus suggests novel nucleolar functions. Mol. Biol. Cell *16*, 260–269.

Pontes, O., Lawrence, R.J., Neves, N., Silva, M., Lee, J.-H., Chen, Z.J., Viegas, W., and Pikaard, C.S. (2003). Natural variation in nucleolar dominance reveals the relationship between nucleolus organizer chromatin topology and rRNA gene transcription in Arabidopsis. Proc. Natl. Acad. Sci. USA *100*, 11418–11423.

Pontes, O., Li, C.F., Nunes, P.C., Haag, J., Ream, T., Vitins, A., Jacobsen, S.E., and Pikaard, C.S. (2006). The *Arabidopsis* chromatin-modifying nuclear siRNA pathway involves a nucleolar RNA processing center. Cell *126*, this issue, 79–92.

Pontier, D., Yahubyan, G., Vega, D., Bulski, A., Saez-Vasquez, J., Hakimi, M.A., Lerbs-Mache, S., Colot, V., and Lagrange, T. (2005). Reinforcement of silencing at transposons and highly repeated sequences requires the concerted action of two distinct RNA polymerases IV in Arabidopsis. Genes Dev. *19*, 2030–2040.

Schauer, S.E., Jacobsen, S.E., Meinke, D.W., and Ray, A. (2002). DICER-LIKE1: blind men and elephants in Arabidopsis development. Trends Plant Sci. *7*, 487–491.

Shaw, P.J., and Brown, J.W. (2004). Plant nuclear bodies. Curr. Opin. Plant Biol. *7*, 614–620.

Soppe, W.J., Jasencakova, Z., Houben, A., Kakutani, T., Meister, A., Huang, M.S., Jacobsen, S.E., Schubert, I., and Fransz, P.F. (2002). DNA methylation controls histone H3 lysine 9 methylation and heterochromatin assembly in Arabidopsis. EMBO J. *21*, 6549–6559.

Tijsterman, M., Ketting, R.F., and Plasterk, R.H. (2002). The genetics of RNA silencing. Annu. Rev. Genet. *36*, 489–519.

Tran, R.K., Zilberman, D., de Bustos, C., Ditt, R.F., Henikoff, J.G., Lindroth, A.M., Delrow, J., Boyle, T., Kwong, S., Bryson, T.D., et al. (2005). Chromatin and siRNA pathways cooperate to maintain DNA methylation of small transposable elements in Arabidopsis. Genome Biol. *6*, R90.

Vankan, P., and Filipowicz, W. (1988). Structure of U2 snRNA genes of Arabidopsis thaliana and their expression in electroporated plant protoplasts. EMBO J. *7*, 791–799.

Verdel, A., Jia, S., Gerber, S., Sugiyama, T., Gygi, S., Grewal, S.I., and Moazed, D. (2004). RNAi-mediated targeting of heterochromatin by the RITS complex. Science *303*, 672–676.

Volpe, T.A., Kidner, C., Hall, I.M., Teng, G., Grewal, S.I., and Martienssen, R.A. (2002). Regulation of heterochromatic silencing and histone H3 lysine-9 methylation by RNAi. Science *297*, 1833–1837.

Wassenegger, M. (2005). The role of the RNAi machinery in heterochromatin formation. Cell *122*, 13–16.

Xie, Z., Johansen, L.K., Gustafson, A.M., Kasschau, K.D., Lellis, A.D., Zilberman, D., Jacobsen, S.E., and Carrington, J.C. (2004). Genetic and functional diversification of small RNA pathways in plants. PLoS Biol. *2*, e104.

Zilberman, D., Cao, X., and Jacobsen, S.E. (2003). ARGONAUTE4 control of locus-specific siRNA accumulation and DNA and histone methylation. Science *299*, 716–719.

Zilberman, D., Cao, X., Johansen, L.K., Xie, Z., Carrington, J.C., and Jacobsen, S.E. (2004). Role of Arabidopsis ARGONAUTE4 in RNA-directed DNA methylation triggered by inverted repeats. Curr. Biol. *14*, 1214–1220.